

## Electronic Supplementary Information

### **Cu nanoparticles constrain segmental dynamics in cross-linked polyethers: a trade-off between non-fouling and antibacterial properties**

Daniil Nikitin,<sup>a</sup> Sherif Madkour,<sup>b,1</sup> Pavel Pleskunov,<sup>a</sup> Renata Tafiichuk,<sup>a</sup> Artem Shelemin,<sup>a</sup> Jan Hanuš,<sup>a</sup> Ivan Gordeev,<sup>c</sup> Elena Sysolyatina,<sup>d</sup> Alexandra Lavrikova,<sup>d</sup> Svetlana Ermolaeva,<sup>d</sup> Valerii Titov,<sup>e</sup> Andreas Schönals,<sup>\*b</sup> Andrei Choukourov<sup>\*a</sup>

#### **Calculation of $T_g$ from the SHS measurements**

In general, AC-chip calorimetry yields a complex differential voltage as function of temperature and frequency, which is related to the complex heat capacity function, according to equation 1. The real and the imaginary parts of the complex differential voltage are the  $U_R$  and the phase angle  $\phi$ , respectively. The dynamic  $T_g$  could then be calculated as the temperature at half the step-height of the stepwise function of the  $U_R$  and/or the temperature at which the peak function of the  $\phi$  is maximum. It is worth to note that if more than one active process exists, multiple steps or peaks would be expected in the real and the imaginary spectra of the complex differential voltage, respectively. This is seen in Figure S 1 where the real part of the complex differential voltage as well as the corresponding first derivative with respect to temperature are shown for the bi-layered Cu NPs-ppPEO sample with 100nm and 70nm thickness of the ppPEO interlayer.

Here, a recently developed analysis method was employed to estimate the dynamic  $T_g$  with less ambiguity, as described in ref.<sup>1</sup> In this approach, the first derivative, with respect to temperature, of the stepwise function of the real part  $U_R$  is considered. This results in a peak function. Furthermore, a Gaussian (or multiple Gaussian, if needed) is fitted to the peak(s) and the dynamic  $T_g$  is then determined as the maximum temperature at which the peak is maximum. Generally, the AC-chip calorimetry has an error of  $\pm 3$  K. Clearly, both samples in Figure S 1 show the peaks corresponding to the dynamic  $T_g$  of the ppPEO interlayer. However, contrary to the 100 nm sample, the 70 nm sample shows an extra active segmental process observed at higher temperatures.

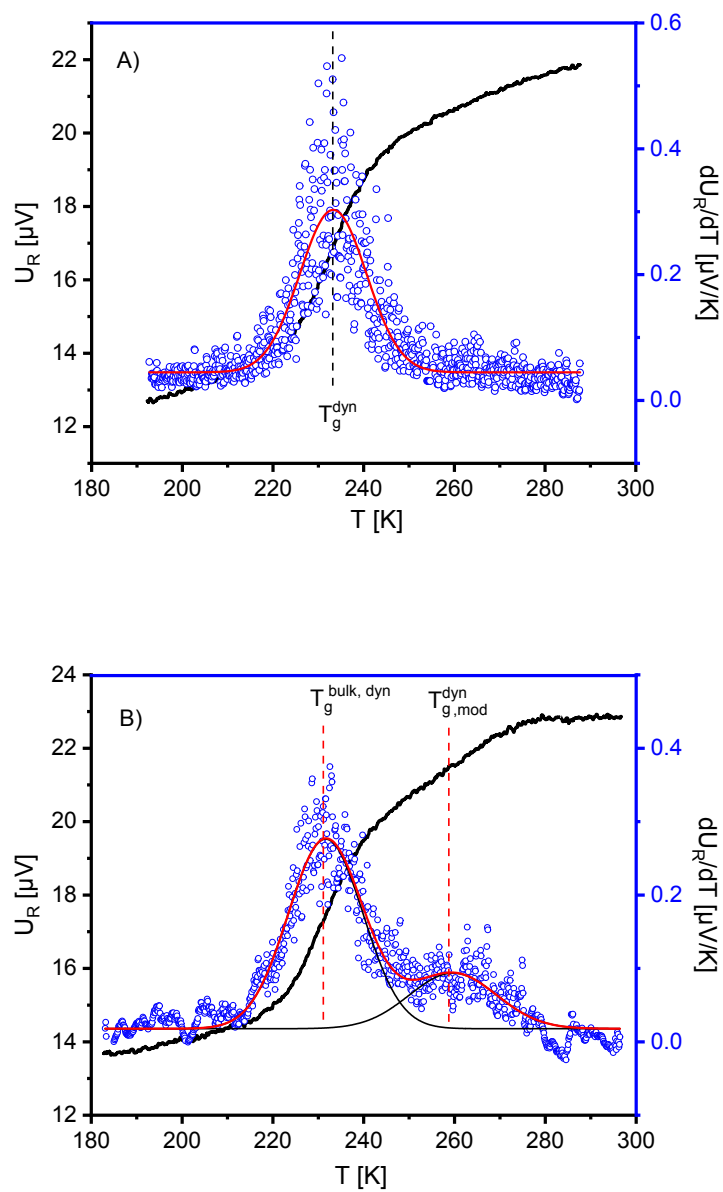


Figure S 1 Real part (black) and the first derivative of the real part (blue circles) of the complex differential voltage versus temperature for bi-layered Cu NPs/ppPEO films with (A)100nm and (B) 70nm thickness of the ppPEO interlayer. The measuring frequency was 160 Hz. The solid red lines are Gaussian fits to the data.

### Calculation of the Cu NP mean size

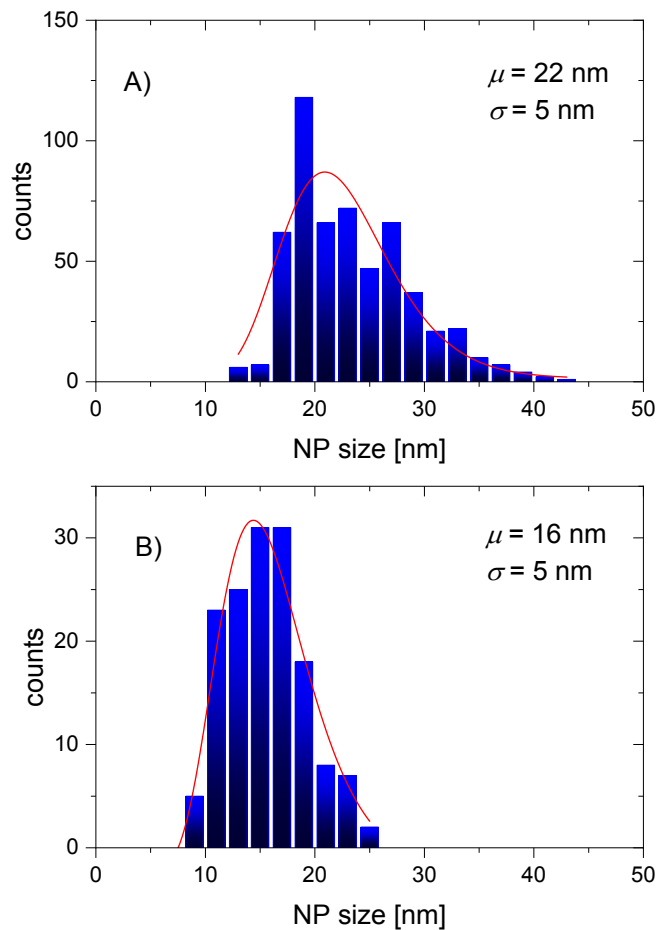


Figure S 2 Size histogram of Cu NPs: A) corresponding to Cu NPs on Si as shown in SEM image of Figure 2; B) corresponding to two sub-monolayer of Cu NPs separated by the 100 nm ppPEO interlayer as shown in TEM image of Figure 4. The histograms are fitted with the lognormal distribution function;  $\mu$  is the mean size and  $\sigma$  is standard deviation.

### Preparation of the bi-layered Cu NPs/ppPEO samples for the SHS analysis

The bi-layered nanocomposite samples were prepared step by step without breaking the vacuum, as follows:

- I. Deposition of a 5 nm film of ppPEO, as an underlying layer.
- II. Deposition of the first layer of Cu NPs with a particle fluence of 250 NPs/ $\mu\text{m}^2$ .
- III. Deposition of the ppPEO interlayer over the first layer of Cu NPs. The thickness of the interlayer was varied between 10 nm and 100 nm.
- IV. Deposition of the second layer of Cu NPs with a particle fluence of 250 NPs/ $\mu\text{m}^2$ .
- V. Deposition of a capping 10 nm ppPEO layer.

### Results of fitting of the relaxation maps by the VFT equation

**Table S 1** Estimated VFT parameters

Interlayer thickness, nm	$\log(f_\infty, \text{Hz})$	$T_0, \text{K}$	D
100	19.95	177.8	2.73
70	14.18	189.1	2.77
40	15.47	194.8	2.65
30	13.71	194.5	2.39
15	7.78	217.0	0.47
10	6.65	223.4	0.29

### References

- 1 S. Madkour, H. Yin, M. Füllbrandt and A. Schönhals, *Soft Matter*, 2015, **11**, 7942–7952.